

## 2-Pentadecyl-2-oxazoline inhibits lipopolysaccharide-induced microglia activation interfering with TLR4 signaling

Laura Facci<sup>a</sup>, Chiara Bolego<sup>a</sup>, Chiara Chemello<sup>a</sup>, Reem Yasser<sup>a</sup>, Mariella Fusco<sup>b</sup>,  
Massimo Barbierato<sup>a</sup>, Pietro Giusti<sup>a</sup>, Stefano Moro<sup>a</sup>, Morena Zusso<sup>a,\*</sup>

<sup>a</sup> Department of Pharmaceutical and Pharmacological Sciences, University of Padua, 35131 Padua, Italy

<sup>b</sup> Scientific Information and Documentation Center, Epitech Group SpA, Padua, Italy

### ARTICLE INFO

#### Keywords:

Neuroinflammation  
Microglia  
2-pentadecyl-2-oxazoline  
Inflammatory cytokines  
TLR4–MD-2 complex

### ABSTRACT

**Aim:** 2-Pentadecyl-2-oxazoline (PEA-OXA), the oxazoline derivative of *N*-palmitoylethanolamine, exerts anti-inflammatory activity; however, very little is known about the molecular mechanisms underlying this effect. Here, we tested the anti-neuroinflammatory effect of PEA-OXA in primary microglia and we also investigated the possible interaction of the molecule with the Toll-like receptor 4 (TLR4)–myeloid differentiation protein-2 (MD-2) complex.

**Main methods:** The anti-inflammatory effect of PEA-OXA was analyzed by measuring the expression and release of pro-inflammatory mediators in primary microglia by real-time PCR and ELISA, respectively. The effect of PEA-OXA on the activation of TLR4 signaling was assessed using two stably TLR4-transfected cell lines (*i.e.*, HEK-293 and Ba/F3 cells). Finally, the putative binding mode of PEA-OXA to TLR4–MD-2 was investigated by molecular docking simulations.

**Key findings:** Treatment with PEA-OXA resulted in the following effects: (i) it down-regulated gene expression of several pro-inflammatory molecules and the secretion of pro-inflammatory cytokines in LPS stimulated microglia cells; (ii) it did not prevent microglia activation after stimulation with TLR2 ligands; (iii) it prevented TLR4/NF- $\kappa$ B activation triggered by LPS in HEK-Blue™ hTLR4 cells; and (iv) it interfered with the binding of LPS to TLR4–MD-2 complex. Furthermore, molecular docking studies suggested that PEA-OXA could bind MD-2 with a 1:3 (MD-2/PEA-OXA) stoichiometry.

**Conclusion:** We show for the first time that the anti-neuroinflammatory effect of PEA-OXA involves its activity against TLR4 signaling, making this molecule a valuable tool for the development of new compounds directed to control neuroinflammation via inhibiting TLR4 signaling.

### 1. Introduction

Microglia are key players in maintaining the central nervous system (CNS) homeostasis due to their ability to sense the environment and protect against modified-self and non-self-injurious agents [1]. Resting microglia are activated in various CNS pathological conditions, such as infection, mechanical injury, and neurodegenerative disease, by endogenous or exogenous mediators including lipopolysaccharide

(LPS),  $\beta$ -amyloid, thrombin, low density lipoproteins, heat-shock proteins, interferon- $\gamma$ , pro-inflammatory cytokines, *etc.* [2]. The primary function of activated microglia is protective: these cells defend the brain against harmful factors and eliminate microbes, dead cells, redundant synapses, protein aggregates, and soluble antigens that may compromise the CNS integrity. However, chronic microglia activation can lead to irreversible CNS damage. Indeed, persistent CNS inflammation affects neuronal plasticity, impairs memory, and is generally considered a

**Abbreviations:** CD14, cluster of differentiation 14; CNS, central nervous system; COX-2, cyclooxygenase-2; DMEM, Dulbecco's modified eagle medium; DMSO, dimethyl sulfoxide; FBS, fetal bovine serum; IL, interleukin; iNOS, inducible nitric oxide synthase; LDH, lactate dehydrogenase; LPS, lipopolysaccharide; MD-2, myeloid differentiation protein-2; MOE, molecular operation environment program; NAEs, *N*-acylethanolamines; Pam<sub>3</sub>CSK<sub>4</sub>, Pam3CysSerLys<sub>4</sub>; PDB, protein data bank; PEA, palmitoylethanolamide; PEA-OXA, 2-pentadecyl-2-oxazoline; PCR, polymerase chain reaction; PPAR, peroxisome proliferator-activated receptor; rms, root-mean-square; SEM, standard error of the mean; TLR, toll-like receptor; TNF- $\alpha$ , tumor necrosis factor- $\alpha$ .

\* Corresponding author at: Department of Pharmaceutical and Pharmacological Sciences, University of Padua, Largo E. Meneghetti 2, 35131 Padua, Italy.

E-mail address: [morena.zusso@unipd.it](mailto:morena.zusso@unipd.it) (M. Zusso).

<https://doi.org/10.1016/j.lfs.2023.122242>

Received 14 June 2023; Received in revised form 24 October 2023; Accepted 1 November 2023

Available online 10 November 2023

0024-3205/© 2023 The Authors. Published by Elsevier Inc. This is an open access article under the CC BY-NC-ND license (<http://creativecommons.org/licenses/by-nc-nd/4.0/>).

typical driver of tissue damage in neurodegenerative disorders. Microglia activation is considered either a causal or a contributing factor to almost all brain diseases, from neurodevelopmental to neurodegenerative disorders [3]. Along with microglia, Toll like receptors (TLRs) have substantial roles in immune responses by recognizing pathogen-derived molecules and molecules of endogenous origin resulting from cellular damage [4]. Specifically, TLR2 and TLR4 are abundantly expressed by microglia and are the most studied TLRs in the context of neuro-inflammation and neurodegeneration [5]. These considerations make microglia and TLRs suitable targets for therapies aimed at restoring homeostasis of the brain parenchyma.

Homeostatic microglia synthesize the endocannabinoids 2-arachidonoylglycerol and anandamide as well as N-acyl-ethanolamines (NAEs) and express their receptors at constitutively low levels [6]. Upon activation, microglia increase the synthesis of endocannabinoids and NAEs and upregulate the expression of their receptors; these events promote a protective microglial phenotype by enhancing the production of neuroprotective factors and reducing that of pro-inflammatory factors [6,7]. Among NAEs, N-palmitoylethanolamine (PEA), which is locally produced on demand from the lipid bilayer, is an autacoid local injury antagonist amide (ALIAmide) [8] with well-known analgesic, anti-inflammatory, antimicrobial, anticonvulsant, immunomodulatory, and neuroprotective properties [9–13]. These actions are mediated by direct and indirect interactions of PEA with different receptors, such as peroxisome proliferator-activated receptor (PPAR)- $\alpha$ , orphan G-protein-coupled receptor 55, CB1 and CB2 receptors, and the transient receptor potential vanilloid 1 [14–17]. Furthermore, recent studies have shown that PEA exerts anti-neuroinflammatory effects through the modulation of microglia reactive phenotypes and these effects are linked to the direct activation of PPAR- $\alpha$  and to the indirect regulation of CB2 receptors [18,19].

Several studies have revealed that an oxazoline derivative of PEA, the 2-pentadecyl-2-oxazoline (PEA-OXA) exerts stronger anti-nociceptive and anti-inflammatory effects than PEA. PEA-OXA inhibits the PEA-degrading enzyme N-acyl-ethanolamine-hydrolyzing acid amidase, and thus increases levels and actions of endogenous PEA [20–22]. Furthermore, more recently, PEA-OXA has been described as an  $\alpha_2$  adrenergic receptor antagonist and a modulator of histamine H3 receptors [23,24]. However, to date the mechanism and the molecular target(s) of the anti-inflammatory activity of PEA-OXA have not been determined.

The present study was designed to investigate whether PEA-OXA was able to attenuate LPS-induced microglia activation and it includes experiments aimed at exploring molecular mechanisms responsible for PEA-OXA effects.

## 2. Materials and methods

### 2.1. Materials

Unless otherwise specified, all chemicals, tissue culture media, and antibiotics were from Merck (Milan, Italy). Fetal bovine serum (FBS) was obtained from Life Technologies (San Giuliano Milanese, Italy). LPS (Ultrapure LPS-EB from *Escherichia Coli*, 0111:B4 strain) and biotinylated LPS (LPS-EB Biotin from *Escherichia Coli*, 0111:B4) were purchased from InvivoGen (InvivoGen Europe, Toulouse, France); these ultrapure preparations only activate TLR4. CLI-095, an inhibitor of TLR4 signaling, LPS-RS (Ultrapure LPS from *Rhodobacter sphaeroides*), a potent antagonist of TLR4, Pam3CysSerLys4 (Pam<sub>3</sub>CSK<sub>4</sub>), an activator of the TLR2/TLR1 heterodimer, and zymosan, a TLR2 and dectin-1 agonist, were from InvivoGen. PEA-OXA, kindly provided by Epitech Group (Saccolongio, Italy), was dissolved in dimethyl sulfoxide (DMSO)/ethanol (70/30 v/v) and used with a final concentration of 0.07 % DMSO and 0.03 % ethanol. Control cultures contained the same concentration of DMSO and ethanol. Mouse and rabbit anti-GFP (#NB600–597 and #NB600–308) primary antibodies were from Novus, Littleton, CO, USA.

Horseradish peroxidase (HRP)-conjugated secondary antibody was from Bio-Rad Laboratories (Hercules, CA, USA). Falcon tissue culture plasticware were purchased from BD Biosciences (SACCO srl, Cadorago (CO), Italy).

### 2.2. Target structures

Similar to what was reported in our previous computational studies [25,26], the crystallographic structure of the human TLR4-human 1D-2-*E. coli* LPS ternary complex was retrieved from the Protein Data Bank (PDB code: 3FXI) [27]. The assessment of crystallographic structure quality has been performed with the Structure Preparation tool of the Molecular Operation Environment program (MOE, version 2022.02; Chemical Computing Group ULC, 1010 Sherbooke St. West, Suite #910, Montreal, QC, Canada, H3A 2R7, 2023). Critical structural issues (such as missing or poorly resolved atomic data, anomalous topological properties present in amino acids units as well as anomalous bonding patterns of non-amino acids units) were fixed when necessary. Hydrogen atoms were added, and their appropriate protonation state was fixed using the Protonate3D tool as implemented in the MOE program. To minimize contacts between hydrogen atoms, the structures were subjected to Amber99 force field [28] minimization until the root-mean-square (*rms*) of the conjugate gradient was  $<0.1 \text{ kcal mol}^{-1} \text{ \AA}^{-1}$  keeping the heavy atoms fixed at their crystallographic positions.

### 2.3. Molecular docking protocol

PEA-OXA was built using the “Builder” module of MOE, and the compound was docked into the presumptive binding sites (LPS binding site) using flexible MOE-Dock methodology. The purpose of MOE-Dock is to search for favorable binding configurations between a small, flexible ligand and a rigid macromolecular target. Searching is conducted within a user-specified 3D docking box, using the “tabu search” [29] protocol and the MMFF94 force field [30]. Charges for ligands were imported from the MOPAC program [31] output files. MOE-Dock performs a user-specified number of independent docking runs (50 in the present case) and writes the resulting conformations and their energies to a molecular database file. The resulting ligand/protein complexes were subjected to MMFF94 all-atom energy minimization until the *rms* of conjugate gradient was  $<0.1 \text{ kcal mol}^{-1} \text{ \AA}^{-1}$ . GB/SA approximation [32] was used to model the electrostatic contribution to the free energy of solvation in a continuum solvent model. The interaction energy values were calculated as the energy of the complex minus the energy of the ligand, minus the energy of the protein:  $\Delta E_{\text{inter}} = E_{\text{(complex)}} - (E_{\text{(L)}} + E_{\text{(Protein)}})$ .

### 2.4. Cell cultures

Sprague-Dawley rats (CD strain) were maintained under controlled temperature and humidity, with free access to water and food on a 12-h light/dark cycle (lights on at 7:00 am). Animal-related procedures followed Italian Ministry of Health guidelines (D.L. 26/2014) for the care and use of laboratory animals and were approved by the Institutional Review Board for Animal Research (Organismo Preposto al Benessere Animale, OPBA) of the University of Padua and by the Italian Ministry of Health (protocol number 41451.N.N8P). Primary microglial cells were isolated from mixed glial cell cultures prepared from cerebral cortices of PN1 rat pups, as previously described [33]. In brief, when mixed glial cultures reached confluence (typically 7 days after isolation), microglia were recovered by shaking the flasks on an orbital shaker (200 rpm for 1 h at 37 °C), re-suspended in high-glucose Dulbecco's modified eagle medium (DMEM) supplemented with 2 mM L-glutamine, 10 % heat-inactivated FBS, 100 units/ml penicillin, 100 µg/ml streptomycin, and 50 µg/ml gentamicin (growth medium), transferred to Sterilin plastic Petri dishes, and incubated for 45 min at 37 °C (5 % CO<sub>2</sub>, 95 % air) to allow adhesion of microglia. The adherent microglial cells (> 99 % pure,

as determined by flow cytometry using cell type-specific antibodies [34]) were detached by mechanically scraping into growth medium and re-plated in this same medium, on poly-L-lysine-coated plastic wells at a density of  $1.50 \times 10^5$  cells/cm<sup>2</sup>.

HEK-Blue™ hTLR4 cells, obtained by co-transfection of the human TLR4, MD-2 and cluster of differentiation 14 (CD14) co-receptor genes, and an NF-κB-inducible secreted embryonic alkaline phosphatase (SEAP) reporter gene into human embryonic kidney 293 (HEK293) cells, were purchased from InvivoGen. Cells were cultured in high-glucose DMEM supplemented with 2 mM L-glutamine, 10 % FBS, 100 units/ml penicillin, 100 µg/ml streptomycin, 100 µg/ml normocin™ (InvivoGen) and 1 × HEK-Blue™ selection (InvivoGen) (selection medium), according to the supplier's instructions. When the cells reached the confluency of ~80 %, they were subcultured and plated at a density of  $0.1 \times 10^6$  cells/ml.

Murine Ba/F3 cells, an interleukin (IL)-3 dependent pro-B cell line, stably expressing human TLR4-GFP, human TLR4-Flag, human MD-2-Flag, and human CD14 were kindly provided by Dr. Kensuke Miyake (University of Tokyo, Japan). Cells were cultured in RPMI1640 medium, supplemented with 10 % FBS, 100 µM 2-mercaptoethanol, and recombinant murine IL-3 (~70 U/ml) [35].

Cells were maintained at 37 °C in a humidified atmosphere containing 5 % CO<sub>2</sub>/95 % air.

## 2.5. Microglia viability assay

Microglia were seeded in poly-L-lysine coated 96-well plates in growth medium and allowed to adhere overnight. Growth medium was replaced with serum-free medium and cells were exposed to increasing concentrations of PEA-OXA (0.1–30 µM) for 24 h. After the incubation period, the medium was removed for lactate dehydrogenase (LDH) release assay, using the CytoTox® non-radioactive cytotoxicity assay kit (Promega Corporation, Madison, WI, USA) following the manufacturer's protocol. The relative absorbance of all samples was measured at 490 nm with a microplate reader (Victor2 Multilabel Counter, Wallac, Cambridge, MA, USA).

## 2.6. Cell reporter assay

HEK-Blue™ hTLR4 cells were plated at a density of  $0.4 \times 10^5$  cells per well using 200 µl/well (96-well-plate) of selection medium and allowed to adhere overnight. Selection medium was replaced with serum-free medium, and cells were pretreated for 1 h with increasing concentrations of PEA-OXA (0.1–30 µM), CLI-095 (0.5 µg/ml), or LPS-RS (100 ng/ml) and then stimulated with 5 ng/ml Ultra-Pure LPS-EB for 24 h. Supernatants were collected and SEAP released in the culture medium was quantified using the QUANTI-Blue™ Solution (InvivoGen). Briefly, 20 µl of supernatants were incubated with 180 µl of the QUANTI-Blue™ Solution in a 96-well plate for 15 min. SEAP activity, as an indicator of TLR4 activation, was assessed by reading the optical density at 630 nm (OD<sub>630</sub>) with a microplate reader.

## 2.7. Cytokine determination

Primary microglia were pretreated for 1 h with 30 µM PEA-OXA and then stimulated with 100 ng/ml Ultra-Pure LPS-EB, 300 ng/ml Pam<sub>3</sub>CSK<sub>4</sub>, or 10 µg/ml zymosan for additional 6 or 24 h. At the end of incubation, culture medium was collected and IL-1β and tumor necrosis factor (TNF)-α assayed using commercially available ELISA kits (Antigenix America, Huntington Station, NY, USA), according to the manufacturer's instructions. The absorbance of each sample was detected at 450 nm with a microplate reader. Cytokine concentrations (pg/ml) in the medium were determined by reference to standard curves obtained with known amounts of IL-1β or TNF-α.

## 2.8. Immunoprecipitation and western blotting

Immunoprecipitation experiments were performed using Ba/F3 cells stably expressing human TLR4-GFP, human TLR4-Flag, human MD-2-Flag, and human CD14. Ba/F3 cells ( $80 \times 10^6$  cells/condition) were pretreated for 1 h with PEA-OXA (30 µM) and then stimulated with 250 ng/ml biotinylated LPS [26,36] for 30 min. Protein extracts were prepared as described previously [35]. The samples were immunoprecipitated with mouse anti-GFP antibody for 16–18 h at 4 °C. The recovered proteins were resolved using 10 % SDS-PAGE and electrotransferred to a nitrocellulose membrane. Membrane was blocked with 3 % bovine serum albumin for 1 h at room temperature and then exposed to streptavidin-HRP (Cell Signaling Technology, Beverly, MA, USA) for 1 h or probed overnight with rabbit anti-GFP antibody, followed by HRP-conjugated secondary antibodies for 1 h, to examine the interference of PEA-OXA with LPS binding to TLR4–MD-2 complex. Reactive bands were visualized with the ECL substrate (GE Healthcare Amersham, UK), using the VersaDoc Imaging System (Bio-Rad Laboratories, USA). Densitometry quantification of bands was performed with ImageJ software and biotinylated-LPS was normalized to TLR4-GFP levels.

## 2.9. Real-time polymerase chain reaction (real-time PCR)

Total RNA was extracted from cells by QIAzol (Invitrogen), according to the manufacturer's instructions. RNA integrity and quantity were determined by RNA 6000 Nano assay (A<sub>260/280</sub> ratio > 1.8) in an Agilent BioAnalyser (Thermo Scientific, Milan, Italy). Reverse transcription was performed with Superscript IV reverse transcriptase (Invitrogen). The real-time PCR reaction was performed as described previously [37]. Primer sequences are listed in Table 1. Amounts of each gene product were calculated using linear regression analysis from standard curves, demonstrating amplification efficiencies ranging from 90 to 100 %. Dissociation curves were generated for each primer pair, showing single product amplification. Data were normalized to β-actin mRNA level and results are reported as fold changes compared to control value.

## 2.10. Statistical analysis

All data represent the results of at least three independent experiments. Statistical analysis was performed using GraphPad Prism Software, version 8.0 (GraphPad Software, Inc., San Diego, CA, USA). Results are expressed as mean ± standard error of the mean (SEM). Data were analyzed by one- or two-way ANOVA followed by Sidak's *post hoc* analysis, when applicable. *P* values <0.05 were considered statistically significant.

## 3. Results

### 3.1. PEA-OXA suppresses LPS-induced inflammatory enzymes in microglia

To explore the activity of PEA-OXA on the neuroinflammatory

**Table 1**  
Primers for real-time PCR used in this study.

Gene target	Primer name	Sequence (5'-3')
COX-2	COX-2 For	TTTCAATGTGCAAGACCCGC
	COX-2 Rev	ACAGCTCAGTTGAACGCCTT
IL-1β	IL-1β For	CGTCCTCTGTGACTCGTGGG
	IL-1β Rev	ATGGGTACAGACGACGAGG
iNOS	iNOS For	GGGAACACCTGGGGATTTC
	iNOS Rev	CACAGTTTGGTCTGGCGAAG
TNF-α	TNF-α For	CGAGGTTCCGTCCTCTCAT
	TNF-α Rev	TGCCAGTTCACATCTCGGA
β-actin	β-actin For	GATCAGCAAGCAGGAGTACGATGA
	β-actin Rev	GGTGAAACGACGCTCAGTAACA

response of microglia, we investigated its effect on the expression of some inflammatory signal messengers in microglia cultures when stimulated with LPS, a TLR4 ligand. Cells were exposed to increasing concentrations (0.1–30  $\mu\text{M}$ ) of PEA-OXA with or without LPS stimulation. While PEA-OXA itself had no effect on the low amounts of inducible nitric oxide synthase (iNOS) and cyclooxygenase-2 (COX-2) expressed in unstimulated microglia, PEA-OXA reduced in a concentration-dependent manner the increased expression of both genes that were induced by a 24-h treatment with LPS (Fig. 1a and b). Furthermore, PEA-OXA did not affect cell viability as determined by the LDH assay at concentrations ranging from 0.1 to 30  $\mu\text{M}$ , suggesting that its inhibitory effect on microglia inflammatory response was not related to nonspecific cytotoxicity (Fig. 1c).

### 3.2. PEA-OXA suppresses cytokine response after challenge with LPS

The inflammatory phenotype of microglia is also characterized by cytokine response, which is known to occur within a few hours after LPS exposure. Specifically, IL-1 $\beta$  and TNF- $\alpha$  are produced early in response to LPS and their dysregulation can lead to pathological damage [38]. To confirm the anti-inflammatory activity of PEA-OXA, we determined the mRNA expression and the release in culture supernatants of IL-1 $\beta$  and TNF- $\alpha$  at two time points (i.e., 6 and 24 h) following LPS stimulation. When tested at the concentration of 30  $\mu\text{M}$ , PEA-OXA significantly reduced the mRNA levels of IL-1 $\beta$  and TNF- $\alpha$ , that were over-expressed after a 6-h LPS exposure (Fig. 2). Changes in gene expression were accompanied by the induction of cytokine release in the culture medium at 24 h, that was suppressed by treatment with PEA-OXA (Fig. 3). In addition, no effect on cytokine mRNA expression levels and release was observed when microglia were treated with PEA-OXA alone, i.e., in the absence of LPS, as compared to vehicle-treated cells (Figs. 2 and 3).

### 3.3. PEA-OXA fails to suppress cytokine response after challenge with TLR2 ligands

Next, we investigated the impact of TLR2 on the anti-neuroinflammatory activity of PEA-OXA. To this end, TLR2 signaling was activated by exposing microglia to Pam<sub>3</sub>CSK<sub>4</sub> (Fig. 4a and b) or zymosan (Fig. 4c and d), two TLR2 ligands that induce the receptor to form TLR2-TLR1 and TLR2-TLR6 heterodimers, respectively. As expected, both ligands markedly increased the release of IL-1 $\beta$  and TNF- $\alpha$ , but PEA-OXA failed to elicit cytokine changes at any time points (Fig. 4). Overall, these results indicate that PEA-OXA inhibits TLR4-mediated inflammatory response of microglia, but not that mediated by TLR2.

### 3.4. PEA-OXA suppresses TLR4 activation and interferes with the formation of the TLR4–MD-2–LPS complex

To gain further insights into the mechanism implicated in the anti-neuroinflammatory effect of PEA-OXA, and especially to clarify the role of TLR4 in mediating this effect, we used a commercially engineered TLR4 reporter cell system (HEK-Blue™ hTLR4 cells) designed to study the stimulation of TLR4 by monitoring the activation of NF- $\kappa\text{B}$ . Activation of NF- $\kappa\text{B}$  induces the production and secretion of SEAP, which can be detected in the culture medium. HEK-Blue™ hTLR4 cells were treated with increasing concentrations of PEA-OXA (0.1–30  $\mu\text{M}$ ) and then stimulated with 5 ng/ml LPS. The stimulation of the cells with LPS yielded a robust release of SEAP in the culture medium. This effect was decreased by the highest concentrations of PEA-OXA (10 and 30  $\mu\text{M}$ ; Fig. 5a), indicating that the compound acts through TLR4. To rule out the presence of contaminants responsible for the induction of TLR4 activation, we used the TLR4 antagonist LPS-RS and the TLR4 specific inhibitor CLI-095, which binds to the intracellular domain of TLR4, preventing downstream pro-inflammatory effects [39–41]. As expected, the LPS-induced SEAP release was not observed when LPS-RS (100 ng/ml) or CLI-095 (0.5  $\mu\text{g}/\text{ml}$ ) were used (green and gray bar in Fig. 5a).

The toxicity of PEA-OXA was also assessed in HEK-Blue™ hTLR4 cells and all the concentrations tested (0.1–30  $\mu\text{M}$ ) showed no cytotoxic effect (Fig. S1).

These findings led us to ask whether PEA-OXA can prevent the formation of the LPS–TLR4–MD-2–LPS complex, which is one of the steps required for the activation of inflammatory response mediated by TLR4 signaling pathway [27]. To address this issue, biotinylated LPS was added to Ba/F3 cells stably expressing TLR4-Flag, TLR4-GFP, MD-2-Flag, and CD14 [35] and the amount of co-immunoprecipitated LPS and TLR4 was determined by immunoblot analysis. Whereas PEA-OXA treatment did not affect the levels of precipitated TLR4-GFP, the amount of biotinylated LPS bound to TLR4–MD-2 was decreased by PEA-OXA (Fig. 5b). These results indicate that PEA-OXA can inhibit the association of biotinylated LPS with TLR4–MD-2 complex, suggesting that its effect against the TLR4–MD-2-mediated inflammatory response could be contingent on its ability to interfere with the binding of LPS to the receptor complex.

### 3.5. Molecular modeling studies of PEA-OXA binding to TLR4–MD-2 complex

The above observations prompted us to explore the potential ability of PEA-OXA to interact with TLR4–MD-2. A molecular docking study was undertaken to analyze the possibility for PEA-OXA to be recognized and stably accommodated in the LPS recognition site of MD-2 structure. For this purpose, we used the crystallographic structure coded by PDB as 3FXI [25,27] (Fig. 6) and our computational study supported the hypothesis that PEA-OXA can find energetically favorable accommodation within the LPS recognition site in MD-2. As expected, the hydrocarbon chain of the PEA-OXA molecule established van der Waals interactions in analogy to what was observed for LPS molecules. Furthermore, if a Mg<sup>2+</sup> ion is present in the TLR4–MD2–LPS ternary complex, as shown in the crystallographic structure used in the present study (Fig. 6), PEA-OXA can stabilize its coordination sphere. As depicted in detail in Fig. 7, the coordination of the Mg<sup>2+</sup> ion can occur through the dative covalent bond which is formed between the metal center and the lone pair of the nitrogen atom of the 2-oxazoline moiety. The simultaneous presence of the alkyl chain-mediated van der Waals interactions within the recognition site of LPS and the coordination of the magnesium cation stabilized the recognition of PEA-OXA against MD-2, making this compound a competitive ligand of LPS.

Furthermore, by carefully looking at the arrangement of the alkyl chains of LPS within its recognition site in MD-2 (see Fig. 6), it is evident that the recognition stoichiometry of PEA-OXA could be higher than 1:1, as the cavity is large enough to accommodate more than one molecule at the same time. To support this hypothesis, the previously described molecular docking procedure was repeated in the presence of a first PEA-OXA molecule already present in the recognition site. The second molecule in its energetically more stable positioning was then subjected to a subsequent docking step confirming that the cavity is large enough to accommodate at least three molecules of PEA-OXA, simultaneously, as shown in Fig. 8.

## 4. Discussion

TLRs are involved in a plethora of physiological and pathological processes. Their activation, especially that of TLR2 and TLR4, is receiving growing interest as being implicated in numerous neurodegenerative and neurological diseases [42,43]. In the CNS, TLRs are differently expressed in astrocytes, oligodendrocytes, microglia, and neurons. Microglia, in particular, besides expressing various immune receptors, express a wide repertoire of TLRs with TLR2 and TLR4 being expressed constitutively at high levels [44]. Expression and activation of TLRs in microglia control the activity and alter the phenotype of these cells, contributing to the evolution of neurodegenerative processes [45]. Thus, TLRs could represent important pharmacological targets for the



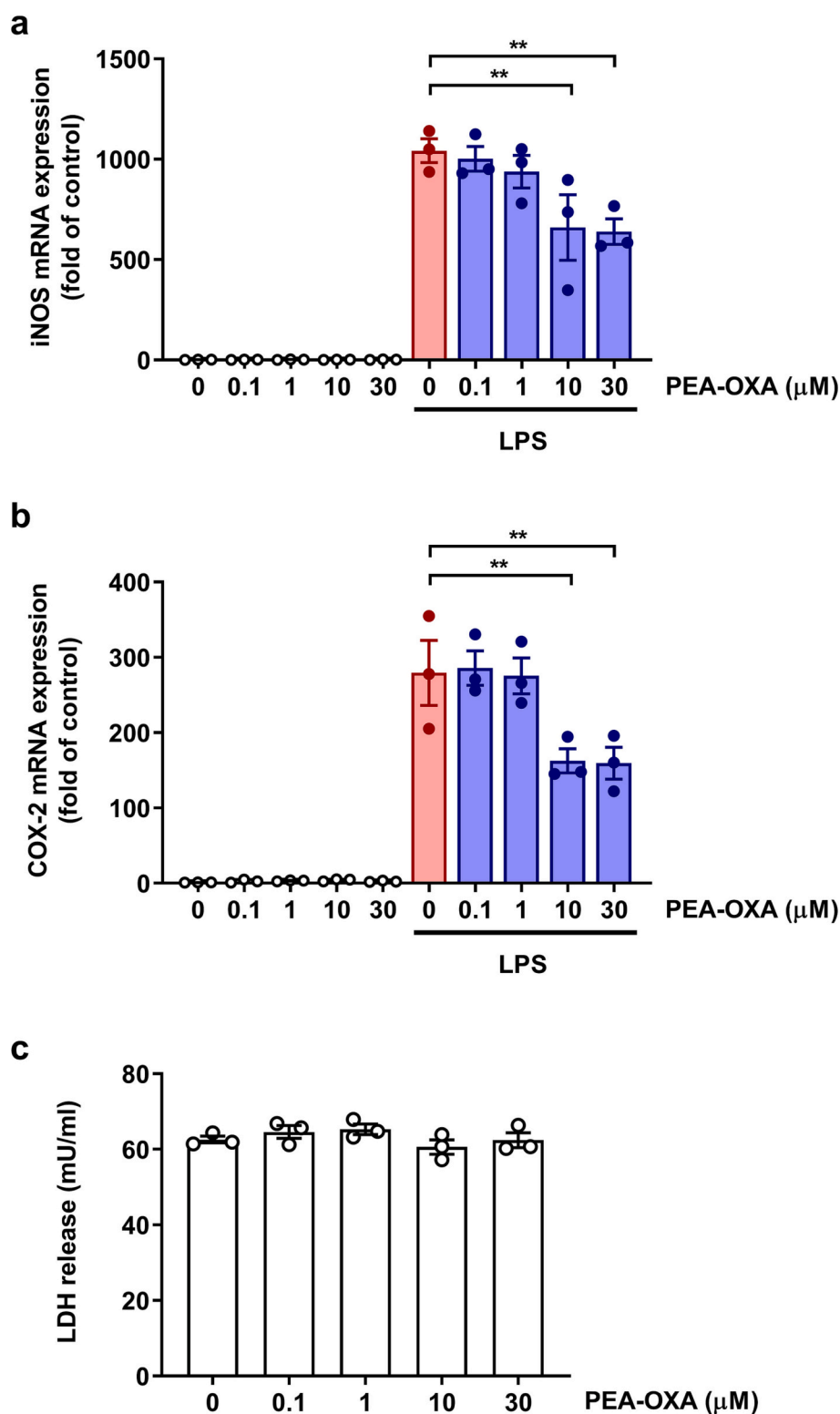


**Fig. 1.** Effect of PEA-OXA on iNOS and COX-2 gene expression in LPS-stimulated cortical microglia and cell viability analysis. Microglia were cultured in 10 % serum-containing medium, which was replaced with serum-free medium before treatment with PEA-OXA (0.1–30  $\mu\text{M}$ ) for 1 h and further stimulation with 100 ng/ml LPS for 24 h. (a) iNOS and (b) COX-2 mRNA levels were quantified by real-time PCR. (c) At the end of 24-h incubation with PEA-OXA (0.1–30  $\mu\text{M}$ ), cell viability was determined by the LDH assay. Data are shown as means  $\pm$  SEM ( $n = 3$  in triplicate) and analyzed by one-way ANOVA followed by Sidak's multiple comparison test. \*\* $p < 0.01$ .

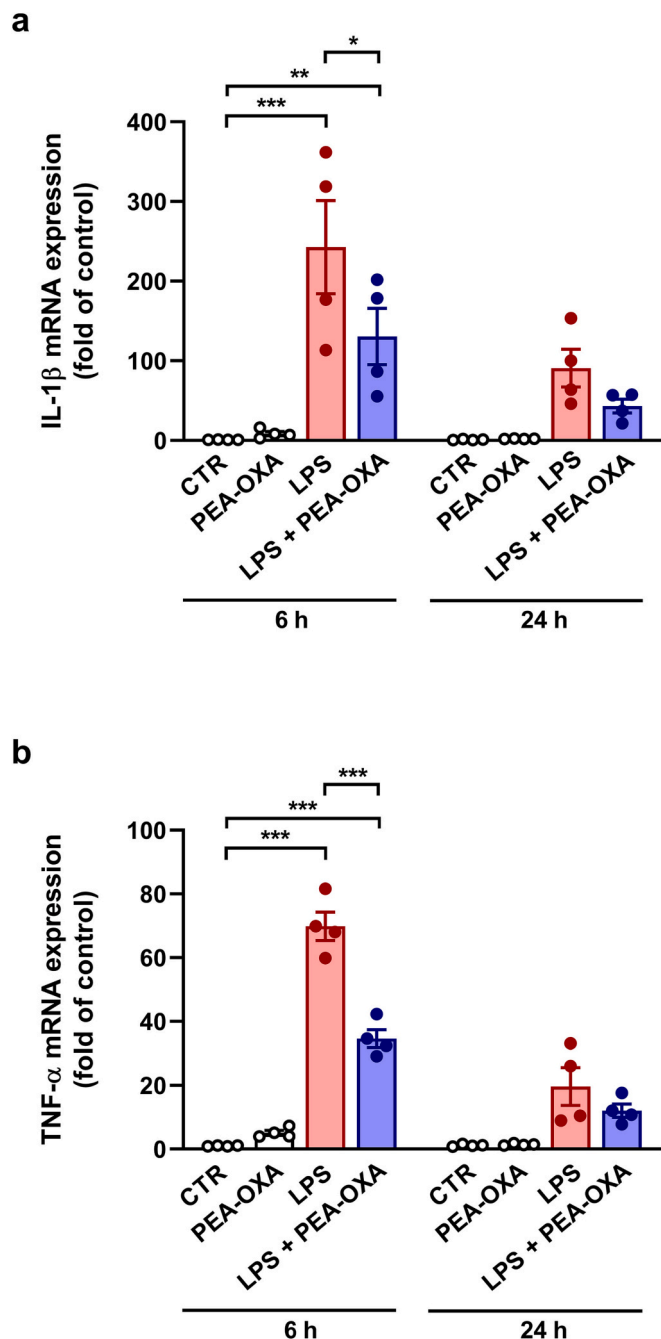


**Fig. 2.** Effect of PEA-OXA on IL-1 $\beta$  and TNF- $\alpha$  gene expression in LPS-stimulated cortical microglia. Microglia were cultured in 10 % serum-containing medium, which was replaced with serum-free medium before treatment with PEA-OXA (30  $\mu$ M) for 1 h and further stimulation with 100 ng/ml LPS for 6 or 24 h. (a) IL-1 $\beta$  and (b) TNF- $\alpha$  mRNA levels were quantified by real-time PCR. Results are shown as means  $\pm$  SEM ( $n = 4$  in triplicate) and analyzed by two-way ANOVA followed by Sidak's multiple comparison test. \* $p < 0.05$ , \*\* $p < 0.01$ , and \*\*\* $p < 0.001$ .

development of compounds aimed at blocking neuroinflammation and microglia activation.

To this purpose, the present study was aimed at investigating whether PEA-OXA would exhibit anti-inflammatory properties in microglia cells by interfering with TLR signaling. PEA-OXA is a natural anti-inflammatory compound, which inhibits the catabolic enzyme *N*-acyl-ethanolamine-hydrolyzing acid amidase, leading to increased levels of the endogenous lipid PEA [20–22]. The latter possesses

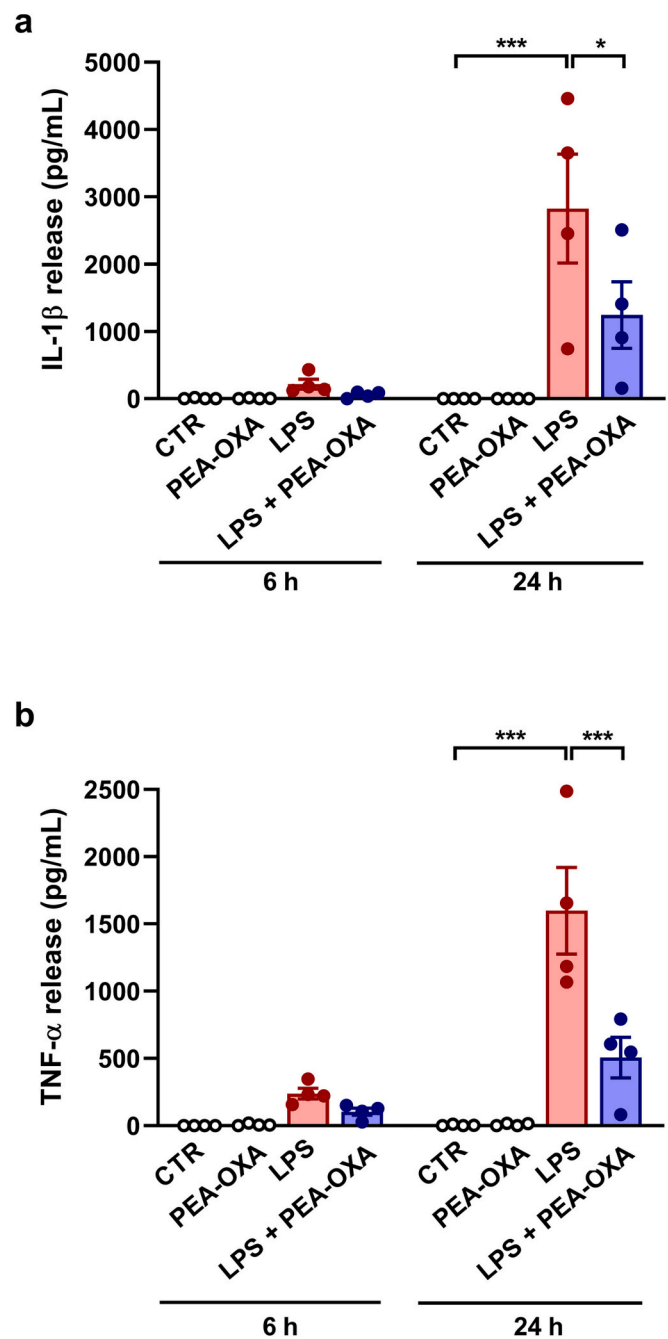


**Fig. 3.** Effect of PEA-OXA on cytokine release from LPS-stimulated cortical microglia. Microglia were cultured in 10 % serum-containing medium, which was replaced with serum-free medium before treatment with PEA-OXA (30  $\mu$ M) for 1 h and further stimulation with 100 ng/ml LPS for 6 or 24 h. Supernatants were collected and analyzed for (a) IL-1 $\beta$  and (b) TNF- $\alpha$  release. Results are shown as means  $\pm$  SEM ( $n = 4$  in triplicate) and analyzed by two-way ANOVA followed by Sidak's multiple comparison test. \* $p < 0.05$  and \*\*\* $p < 0.001$ .

numerous biological activities, including anti-inflammatory effects that are dependent, although not exclusively, on PPAR- $\alpha$  activation [14,46]. Differently, the anti-inflammatory effect of PEA-OXA was unchanged in PPAR- $\alpha$  knockout mice, suggesting different and/or additional mechanisms and/or sites of action of PEA-OXA [21]. Our results show that PEA-OXA decreased LPS-induced microglia activation by reducing the production of pro-inflammatory signals. In particular, the present findings show the capacity of PEA-OXA to down-regulate the LPS-induced gene expression of iNOS, COX-2, IL-1 $\beta$  and TNF- $\alpha$  and the enhanced

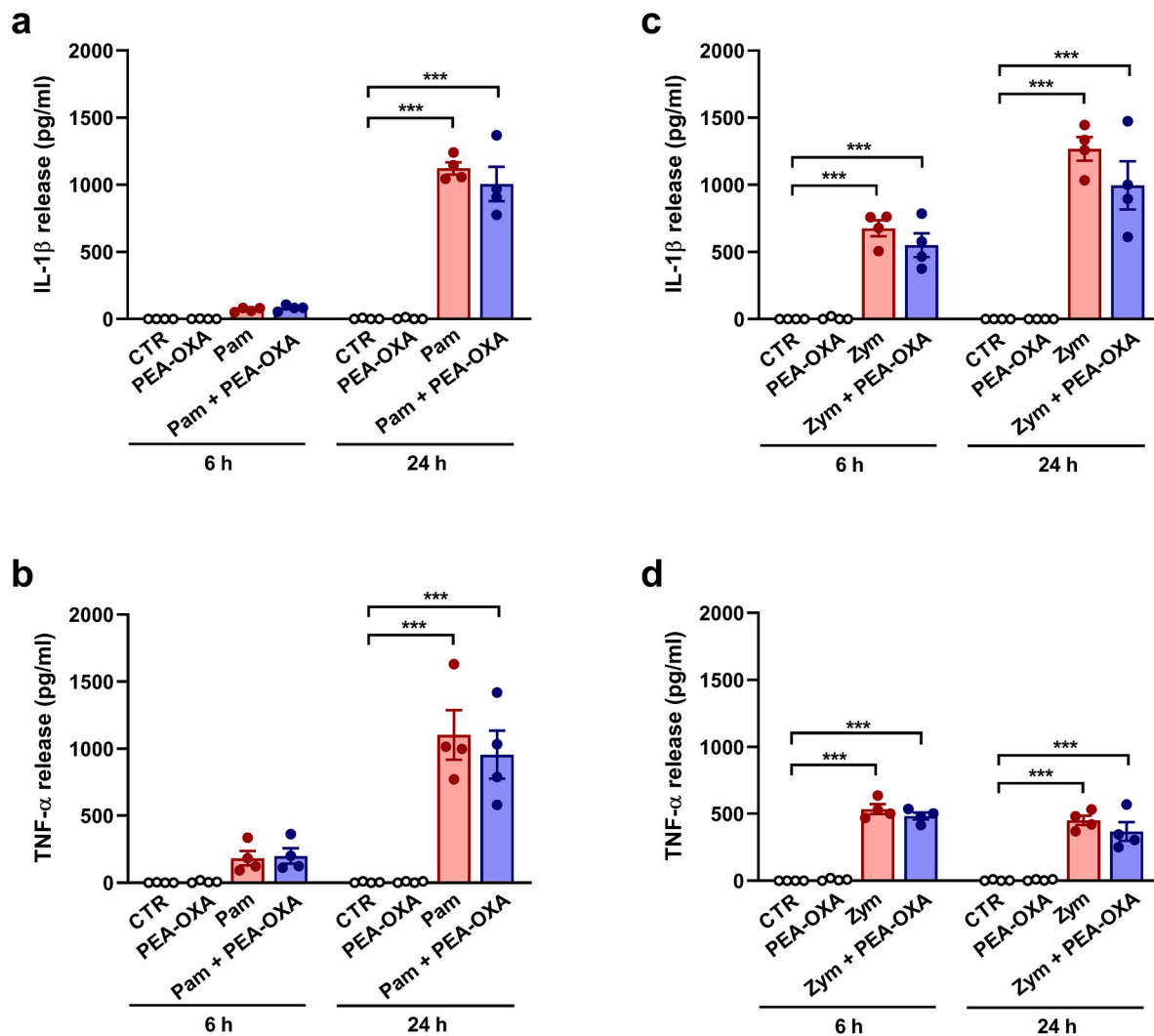


**Fig. 4.** Effect of PEA-OXA on cytokine release from cortical microglia stimulated with TLR2 ligands. Microglia were cultured in 10 % serum-containing medium, which was replaced with serum-free medium before treatment with PEA-OXA (30  $\mu$ M) for 1 h and further stimulation with (a and b) 300 ng/ml Pam<sub>3</sub>CSK<sub>4</sub> (Pam) or (c and d) 10  $\mu$ g/ml zymosan (Zym) for 6 or 24 h. Supernatants were collected and analyzed for (a and c) IL-1 $\beta$  and (b and d) TNF- $\alpha$  release. Results are shown as means  $\pm$  SEM (n = 4 in triplicate) and analyzed by two-way ANOVA followed by Sidak's multiple comparison test. \*\*\*p < 0.001.

release of IL-1 $\beta$  and TNF- $\alpha$ . Considering that LPS is essentially recognized by TLR4 and that the ultra-pure preparation of LPS used in this study only activates the TLR4 pathway [34], our results indicate that PEA-OXA can inhibit TLR4-mediated inflammatory response of microglia. Interestingly, our results suggest some specificity of PEA-OXA to TLR4 since cytokine release observed after microglia stimulation through the TLR2 agonists Pam<sub>3</sub>CSK<sub>4</sub> or zymosan was not altered by the studied molecule.

To clarify the role of TLR4 in mediating the anti-inflammatory effect of PEA-OXA, we took advantage of two stably TLR4-transfected cell lines (i.e., HEK-293 cell line and Ba/F3 cells), designed to provide sensitive and reliable methods to investigate TLR4 activity without interference by other TLRs [35,47]. The ability of PEA-OXA to interfere with LPS-triggered TLR4 activation was first assessed in HEK-Blue™ hTLR4 cells. These cells have been modified to study the activation of TLR4 by monitoring NF- $\kappa$ B activation in terms of SEAP release in the culture medium. Using this approach, we show that TLR4/NF- $\kappa$ B activation triggered by LPS can be prevented by PEA-OXA, corroborating our hypothesis that this molecule has inhibitory activity on TLR4 signaling.

The activation of TLR4 by LPS is a complex and multistep process that requires the binding of LPS monomers to LPS-binding protein, then to CD14 and, ultimately, to MD-2, which forms a complex with TLR4 on

the cell membrane [27]. The binding of LPS to MD-2 causes the TLR4-MD-2 complex dimerization, thereby triggering the activation of downstream mediators, including the transcription factor NF- $\kappa$ B and the production of pro-inflammatory molecules [27,48]. Accordingly, we used Ba/F3 cells stably transfected with human TLR4, MD-2, and CD14 differently tagged (i.e., GFP and Flag) as a tool to facilitate studying one of the initial steps of TLR4 activation, i.e., the interaction between LPS and cell surface TLR4-MD-2. Co-immunoprecipitation and immunoblot analysis of GFP-TLR4 and biotinylated LPS show that PEA-OXA diminished the association of LPS with TLR4-MD-2 complex.

PEA-OXA is a lipidic molecule featuring a C-15 saturated alkyl chain bound to a 2-oxazoline moiety that is structurally related to the lipid A component of LPS and to others TLR4 ligands, including palmitic acid [49,50]. A recent study has shown that *N*-palmitoyl-D-glucosamine, a natural amide of palmitic acid and glucosamine endowed with the anti-inflammatory properties of its analog PEA and those of glucosamine [51], acts as a TLR4 antagonist by binding the MD-2 domain of TLR4 [52]. Due to the structural similarity of PEA-OXA with the lipid A moiety of LPS, similarly to *N*-palmitoyl-D-glucosamine, we hypothesized that this molecule could exert anti-inflammatory activities by binding to TLR4-MD-2 and by interfering with the proper assembly of the TLR4-MD-2-LPS ternary complex. From a chemical point of view, two

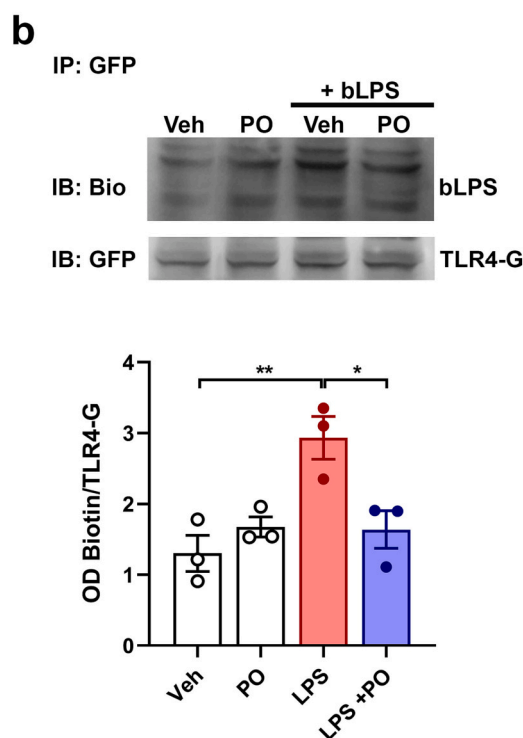
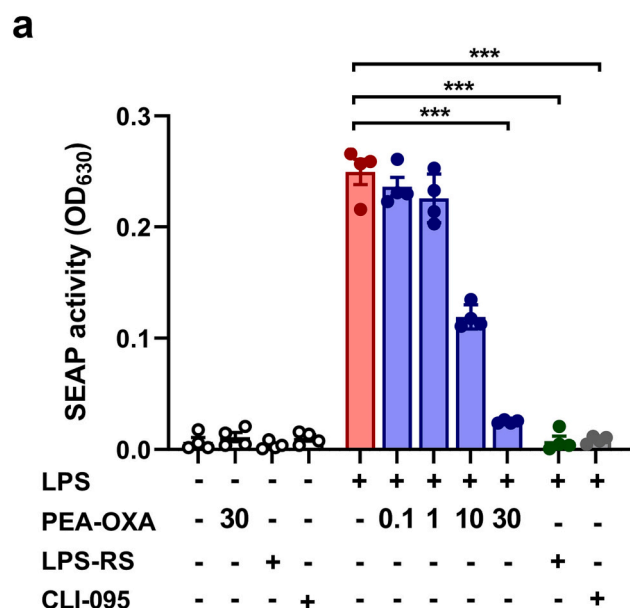


**Fig. 5.** Effects of PEA-OXA on TLR4 activation and LPS binding to TLR4–MD-2 complex. (a) HEK-Blue™ hTLR4 cells were incubated with PEA-OXA (0.1–30  $\mu$ M), LPS-RS (100 ng/ml), or CLI-095 (0.5  $\mu$ g/ml) for 1 h before treatment with 5 ng/ml LPS. The amount of SEAP released into the culture medium was quantified after 24 h. Data are shown as OD<sub>630</sub> and are means  $\pm$  SEM ( $n = 4$ ). (b) Ba/F3 cells expressing TLR4-Flag, TLR4-GFP (TLR4-G), MD2-Flag, and CD14 were incubated with 30  $\mu$ M PEA-OXA (PO) and then stimulated with 250 ng/ml of biotinylated LPS (bLPS). Cell lysates were immunoprecipitated with mouse anti-GFP antibody. The immunoblotted proteins were exposed to streptavidin-HRP (upper lanes) or rabbit anti-GFP antibody (lower lanes). Representative images are shown. The ratio of Biotin-LPS/TLR4-GFP is shown in the graph. Data are means  $\pm$  SEM ( $n = 3$ ). Results were analyzed by one-way ANOVA followed by Sidak's multiple comparison test.  $*p < 0.05$ ,  $**p < 0.01$ ,  $***p < 0.001$ . bLPS, biotinylated LPS; Bio, biotin; IP, immunoprecipitation; IB, immunoblot; PO, PEA-OXA; Veh, vehicle.

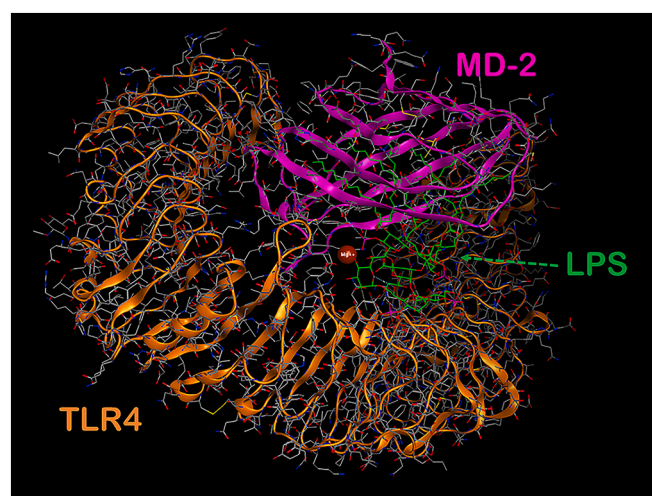


**Fig. 6.** Overall structure of the human TLR4–MD-2–LPS complex derived by the crystallographic structure 3FXI.

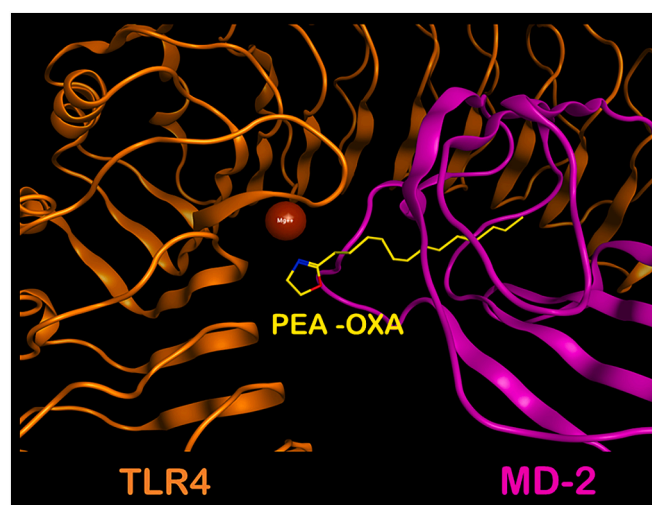


**Fig. 7.** Molecular docking-driven of the energetically more stable binding pose between PEA-OXA and MD-2.

preliminary indications can support the possible mechanism of PEA-OXA competition at the recognition site of LPS in the MD-2 structure: a) the presence of linear aliphatic chains in LPS and PEA-OXA structures; and b) the possibility of coordinating an  $Mg^{2+}$  ion if it is present in the TLR4–MD-2–LPS ternary complex, as shown in the crystallographic structure used in this study, and experimentally demonstrated to play a crucial role in the recognition of diverse TLR4 competitive inhibitors [25,26]. The molecular docking study performed here validated our hypothesis and confirmed that PEA-OXA can stably accommodate in the LPS recognition site in the MD-2 structure with a 1:3 (MD-2/PEA-OXA) stoichiometry. The coordination of the  $Mg^{2+}$  ion through the lone pair of the nitrogen atom of the 2-oxazoline moiety of PEA-OXA could prevent the stabilization of the LPS binding to MD-2, interfering with the TLR4 activation process.

In summary, as far as we know, our study has revealed for the first time a novel mechanism for the anti-neuroinflammatory action of PEA-OXA, based on the inhibition of TLR4 signaling.

## 5. Conclusions

Collectively, in the present study we characterized a mechanism that



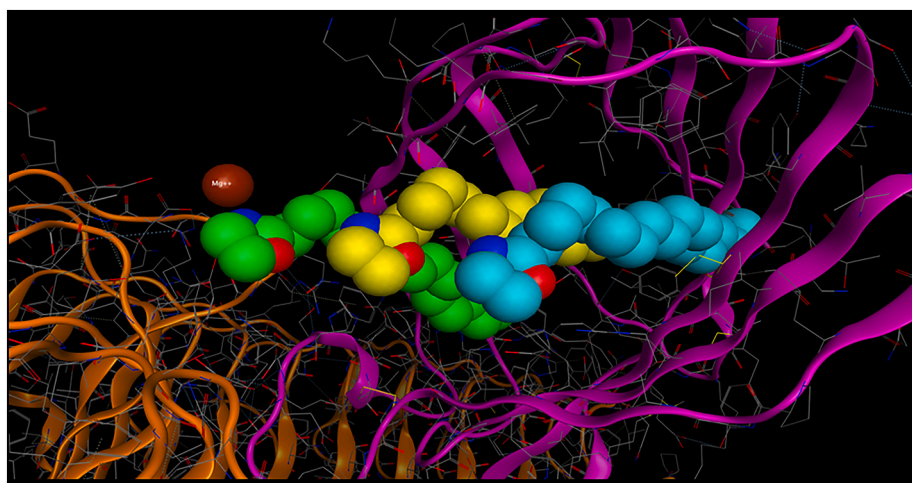


**Fig. 8.** Molecular docking analysis of three-dimensional binding poses between PEA-OXA and MD-2 with stoichiometry 3:1. The LPS binding cavity of MD-2 is zoomed. The three most stable PEA-OXA molecules are shown in the CPK (Corey, Pauling and Koltun) model).

could explain the anti-neuroinflammatory effect of PEA-OXA. We showed that TLR4–MD-2 complex is a novel target for PEA-OXA, that decreases the receptor downstream signal activation and inflammatory mediator expression and release by microglia cells. These findings may provide beneficial information for the development of therapeutic strategies to prevent chronic neuroinflammatory diseases associated with the activation of TLR4 signaling.

#### CRediT authorship contribution statement

LF, CB, PG, SM, and MZ conceived of the study design; LF, CC, RY, MF, MB, SM performed research; LF, CB, PG, SM, MZ analyzed data; SM and MZ wrote the paper; all authors critically revised and approved the final manuscript.

#### Declaration of competing interest

MF was employed by the company Epitech Group SpA. The remaining authors declare that the research was conducted in the absence of any commercial or financial relationships that could be construed as a potential conflict of interest.

#### Data availability

The datasets generated and/or analyzed during the current study are available from the corresponding author on reasonable request.

#### Acknowledgements

We thank Dr. Carla Argentini for technical assistance, Massimo Rizza for technical assistance in animal handling, and Dr. Kensuke Miyake for providing the Ba/F3 cells. SM is very grateful to Chemical Computing Group, OpenEye, and Acellera for their scientific and technical partnership. This study was supported by the Italian Ministry of Economic Development (MISE) - Fund: “Agrifood” PON I&C 2014-2020, referred to the Ministerial Decree March 5, 2018 - Prog no. F/200052/01/X45 and by grants from the University of Padua, Italy (ex 60 % to CB, SM, and MZ).

#### Appendix A. Supplementary data

Supplementary data to this article can be found online at <https://doi.org/10.1016/j.lfs.2023.122242>.

#### References

- [1] S. Hickman, S. Izzy, P. Sen, L. Morsett, J. El Khoury, Microglia in neurodegeneration, *Nat. Neurosci.* 21 (2018) 1359–1369.
- [2] S.C. Woodburn, J.L. Bollinger, E.S. Wohleb, The semantics of microglia activation: neuroinflammation, homeostasis, and stress, *J. Neuroinflammation* 18 (2021) 258.
- [3] M. Cichorek, P. Kowiański, G. Lietzau, J. Lasek, J. Moryś, Neuroglia - development and role in physiological and pathophysiological processes, *Folia Morphol.* 80 (2021) 766–775.
- [4] T. Kawai, S. Akira, The role of pattern-recognition receptors in innate immunity: update on Toll-like receptors, *Nat. Immunol.* 11 (2010) 373–384.
- [5] M.V. Guillot-Sestier, T. Town, Let's make microglia great again in neurodegenerative disorders, *J. Neural Transm.* 125 (2018) 751–770.
- [6] M. Mecha, F.J. Carrillo-Salinas, A. Feliú, L. Mestre, C. Guaza, Microglia activation states and cannabinoid system: therapeutic implications, *Pharmacol. Ther.* 166 (2016) 40–55.
- [7] S.S. Duffy, J.P. Hayes, N.T. Fiore, G. Moalem-Taylor, The cannabinoid system and microglia in health and disease, *Neuropharmacology* 190 (2021), 108555.
- [8] V. Chiurchiù, A. Leuti, R. Smoum, R. Mechoulam, M. Maccarrone, Bioactive lipids ALIAmides differentially modulate inflammatory responses of distinct subsets of primary human T lymphocytes, *FASEB J.* 32 (2018) 5716–5723.
- [9] G. D'Agostino, R. Russo, C. Avagliano, C. Cristiano, R. Meli, A. Calignano, Palmitoylethanolamide protects against the amyloid-β25-35-induced learning and memory impairment in mice, an experimental model of Alzheimer disease, *Neuropsychopharmacology* 37 (2012) 1784–1792.
- [10] R. Citraro, E. Russo, F. Scicchitano, C.M. van Rijn, D. Cosco, C. Avagliano, et al., Antiepileptic action of N-palmitoylethanolamine through CB1 and PPAR-α receptor activation in a genetic model of absence epilepsy, *Neuropharmacology* 69 (2013) 115–126.
- [11] R. Nau, S. Ribes, M. Djukic, H. Eiffert, Strategies to increase the activity of microglia as efficient protectors of the brain against infections, *Front. Cell. Neurosci.* 22 (2014) 138.
- [12] F. Borrelli, B. Romano, S. Petrosino, E. Pagano, R. Capasso, D. Coppola, et al., Palmitoylethanolamide, a naturally occurring lipid, is an orally effective intestinal anti-inflammatory agent, *Br. J. Pharmacol.* 172 (2015) 142–158.
- [13] S. Petrosino, V. Di Marzo, The pharmacology of palmitoylethanolamide and first data on the therapeutic efficacy of some of its new formulations, *Br. J. Pharmacol.* 174 (2017) 1349–1365.
- [14] J. Lo Verme, J. Fu, G. Astarita, G. La Rana, R. Russo, A. Calignano, et al., The nuclear receptor peroxisome proliferator-activated receptor-α mediates the anti-inflammatory actions of palmitoylethanolamide, *Mol. Pharmacol.* 67 (2005) 15–19.
- [15] E. Ryberg, N. Larsson, S. Sjögren, S. Hjorth, N.-O. Hermansson, J. Leonova, et al., The orphan receptor GPR55 is a novel cannabinoid receptor, *Br. J. Pharmacol.* 152 (2007) 1092–1101.
- [16] S.D. Skaper, L. Facci, P. Giusti, Glia and mast cells as targets for palmitoylethanolamide, an anti-inflammatory and neuroprotective lipid mediator, *Mol. Neurobiol.* 48 (2013) 340–352.
- [17] S. Petrosino, A. Schiano Moriello, S. Cerrato, M. Fusco, A. Puigdemont, L. De Petrocellis, et al., The anti-inflammatory mediator palmitoylethanolamide enhances the levels of 2-arachidonoyl-glycerol and potentiates its actions at TRPV1 cation channels, *Br. J. Pharmacol.* 173 (2016) 1154–1162.
- [18] F. Guida, L. Luongo, S. Boccella, M.E. Giordano, R. Romano, G. Bellini, et al., Palmitoylethanolamide induces microglia changes associated with increased migration and phagocytic activity: involvement of the CB2 receptor, *Sci. Rep.* 7 (2017) 375.
- [19] A. D'Alaia, L. Molteni, F. Gullo, E. Bresciani, V. Artusa, L. Rizzi, et al., Palmitoylethanolamide modulation of microglia activation: characterization of

- mechanisms of action and implication for its neuroprotective effects, *Int. J. Mol. Sci.* 22 (2021) 3054.
- [20] D. Impellizzeri, M. Cordaro, G. Bruschetta, R. Crupi, J. Pascali, D. Alfonsi, et al., 2-pentadecyl-2-oxazoline: identification in coffee, synthesis and activity in a rat model of carrageenan-induced hindpaw inflammation, *Pharmacol. Res.* 108 (2016) 23–30.
  - [21] S. Petrosino, M. Campolo, D. Impellizzeri, I. Paterniti, M. Allara, E. Gugliandolo, et al., 2-pentadecyl-2-oxazoline, the oxazoline of pea, modulates carrageenan-induced acute inflammation, *Front. Pharmacol.* 8 (2017) 308.
  - [22] D. Impellizzeri, R. Siracusa, M. Cordaro, R. Crupi, A.F. Peritore, E. Gugliandolo, et al., N-palmitoylethanolamine-oxazoline (PEA-OXA): a new therapeutic strategy to reduce neuroinflammation, oxidative stress associated to vascular dementia in an experimental model of repeated bilateral common carotid arteries occlusion, *Neurobiol. Dis.* 125 (2019) 77–91.
  - [23] S. Boccella, F. Guida, M. Iannotta, F.A. Iannotti, R. Infantino, F. Ricciardi, et al., 2-Pentadecyl-2-oxazoline ameliorates memory impairment and depression-like behaviour in neuropathic mice: possible role of adrenergic  $\alpha$ 2- and H3 histamine autoreceptors, *Mol. Brain* 14 (2021) 28.
  - [24] R. Infantino, S. Boccella, D. Scuteri, M. Perrone, F. Ricciardi, R.M. Vitale, et al., 2-pentadecyl-2-oxazoline prevents cognitive and social behaviour impairments in the amyloid  $\beta$ -induced Alzheimer-like mice model: bring the  $\alpha$ 2 adrenergic receptor back into play, *Biomed. Pharmacother.* 156 (2022), 113844.
  - [25] M. Zusso, G. Mercanti, F. Belluti, R.M.C. Di Martino, A. Pagetta, C. Marinelli, et al., Phenolic 1,3-diketones attenuate lipopolysaccharide-induced inflammatory response by an alternative magnesium-mediated mechanism, *Br. J. Pharmacol.* 174 (2017) 1090–1103.
  - [26] M. Zusso, V. Lunardi, D. Franceschini, A. Pagetta, R. Lo, S. Stifani, et al., Ciprofloxacin and levofloxacin attenuate microglia inflammatory response via TLR4/NF- $\kappa$ B pathway, *J. Neuroinflammation* 16 (2019) 148.
  - [27] B.S. Park, D.H. Song, H.M. Kim, B.S. Choi, H. Lee, J.O. Lee, The structural basis of lipopolysaccharide recognition by the TLR4-MD-2 complex, *Nature* 458 (2009) 1191–1195.
  - [28] W.D. Cornell, P. Cieplak, C.I. Bayly, L.R. Gould, K.M. Merz Jr., D.M. Ferguson, et al., A second generation force field for the simulation of proteins, nucleic acids, and organic molecules, *J. Am. Chem. Soc.* 117 (1995) 5179–5197.
  - [29] C.A. Baxter, C.W. Murray, D.E. Clark, D.R. Westhead, M.D. Eldridge, Flexible docking using Tabu search and an empirical estimate of binding affinity, *Proteins* 33 (1998) 367–382.
  - [30] T.A. Halgren, Merck molecular force field. I. Basis, form, scope, parameterization, and performance of MMFF94, *J. Comput. Chem.* 17 (1996) 490–519.
  - [31] J.J.P. Stewart, MOPAC 7, Fujitsu Limited, Tokyo, Japan, 1993.
  - [32] M. Wojciechowski, B. Lesyng, Generalized born model: analysis, refinement, and applications to proteins, *J. Phys. Chem. B* 108 (2004) 18368–18376.
  - [33] S.D. Skaper, L. Facci, Culture of neonatal rodent microglia, astrocytes, and oligodendrocytes from the cortex, spinal cord, and cerebellum, *Methods Mol. Biol.* 1727 (2018) 49–61.
  - [34] C. Marinelli, R. Di Liddo, L. Facci, T. Beralot, M.T. Conconi, M. Zusso, et al., Ligand engagement of toll-like receptors regulates their expression in cortical microglia and astrocytes, *J. Neuroinflammation* 12 (2015) 244.
  - [35] S. Saitoh, S. Akashi, T. Yamada, N. Tanimura, M. Kobayashi, K. Konno, et al., Lipid A antagonist, lipid IVa, is distinct from lipid A in interaction with toll-like receptor 4 (TLR4)-MD-2 and ligand-induced TLR4 oligomerization, *Int. Immunol.* 16 (2004) 961–969.
  - [36] H. Honda, Y. Nagai, T. Matsunaga, S. Saitoh, S. Akashi-Takamura, H. Hayashi, et al., Glycyrrhizin and isoliquiritigenin suppress the LPS sensor toll-like receptor 4/MD-2 complex signaling in a different manner, *J. Leukoc. Biol.* 91 (2012) 967–976.
  - [37] G. Contarini, D. Franceschini, L. Facci, M. Barbierato, P. Giusti, M. Zusso, A co-ultramicronized palmitoylethanolamide/luteolin composite mitigates clinical score and disease-relevant molecular markers in a mouse model of experimental autoimmune encephalomyelitis, *J. Neuroinflammation* 16 (2019) 126.
  - [38] M.C. Scott, S.S. Bedi, S.D. Olson, C.M. Sears, C.S. Cox, Microglia as therapeutic targets after neurological injury: strategy for cell therapy, *Expert Opin. Ther. Targets* 25 (2021) 365–380.
  - [39] M. Li, N. Matsunaga, K. Hazeki, K. Nakamura, K. Takashima, T. Seya, A novel cyclohexene derivative, ethyl (6R)-6-[N-(2-Chloro-4-fluorophenyl)sulfamoyl]cyclohex-1-ene-1-carboxylate (TAK-242), selectively inhibits toll-like receptor 4-mediated cytokine production through suppression of intracellular signaling, *Mol. Pharmacol.* 69 (2006) 1288–1295.
  - [40] T. Kawamoto, M. Ii, T. Kitazaki, Kimura H. IizawaY, TAK-242 selectively suppresses toll-like receptor 4-signaling mediated by the intracellular domain, *Eur. J. Pharmacol.* 584 (2008) 40–48.
  - [41] A. Piován, R. Filippini, C. Argentin, S. Moro, P. Giusti, M. Zusso, The effect of C-phycocyanin on microglia activation is mediated by toll-like receptor 4, *Int. J. Mol. Sci.* 23 (2022) 1440.
  - [42] S. Amor, M.N. Woodroffe, Innate and adaptive immune responses in neurodegeneration and repair, *Immunology* 141 (2014) 287–291.
  - [43] J. Stephenson, E. Nutma, P. van der Valk, S. Amor, Inflammation in CNS neurodegenerative diseases, *Immunology* 154 (2018) 204–219.
  - [44] M.L. Dallas, D. Widera, TLR2 and TLR4-mediated inflammation in Alzheimer's disease: self-defense or sabotage? *Neural Regen. Res.* 16 (2021) 1552–1553.
  - [45] B.L. Fiebich, C.R.A. Batista, S.W. Saliba, N.M. Yousif, A.C.P. de Oliveira, Role of microglia TLRs in neurodegeneration, *Front. Cell. Neurosci.* 12 (2018) 329.
  - [46] C. Scuderi, G. Esposito, A. Blasio, M. Valenza, P. Arietti, L. Steardo Jr., et al., Palmitoylethanolamide counteracts reactive astrogliosis induced by  $\beta$ -amyloid peptide, *J. Cell. Mol. Med.* 15 (2011) 2664–2674.
  - [47] A. Burger-Kentischer, I.S. Abele, D. Finkelmeier, K.-H. Wiesmüller, S. Rupp, A new cell-based innate immune receptor assay for the examination of receptor activity ligand specificity, signalling pathways and the detection of pyrogens, *J. Immunol. Methods* 358 (2010) 93–103.
  - [48] C.E. Bryant, D.R. Spring, M. Ganglo, N.J. Gay, The molecular basis of the host response to lipopolysaccharide, *Nat. Rev. Microbiol.* 8 (2010) 8–14.
  - [49] R. Cighetti, C. Ciarrelli, S.E. Sestito, I. Zanon, L. Kubik, A. Ardá-Freire, et al., Modulation of CD14 and TLR4, MD-2 activities by a synthetic lipid A mimetic, *Chembiochem* 15 (2014) 250–258.
  - [50] Y. Wang, Y. Qian, Q. Fang, P. Zhong, W. Li, L. Wang, W. Fu, Y. Zhang, Z. Xu, X. Li, G. Liang, Saturated palmitic acid induces myocardial inflammatory injuries through direct binding to TLR4 accessory protein MD2, *Nat. Commun.* 8 (2017) 13997.
  - [51] M. Cordaro, R. Siracusa, D. Impellizzeri, R. D'Amico, A.F. Peritore, R. Crupi, et al., Safety and efficacy of a new micronized formulation of the ALIamide palmitoylglucosamine in preclinical models of inflammation and osteoarthritis pain, *Arthritis Res. Ther.* 21 (2019) 254.
  - [52] M. Iannotta, C. Belardo, M.C. Trotta, F.A. Iannotti, R.M. Vitale, R. Maisto, et al., N-palmitoyl-D-glucosamine, a natural monosaccharide-based glycolipid, inhibits TLR4 and prevents LPS-induced inflammation and neuropathic pain in mice, *Int. J. Mol. Sci.* 22 (2021) 1491.